Magnetoresistance and phase composition of La-Sn-Mn-O systems

Z. W. Li and A. H. Morrish
Department of Physics, University of Manitoba, Winnipeg, Canada R3T 2N2

J. Z. Jiang
Department of Physics, Technical University of Denmark, DK3800, Lyngby, Denmark

(Received 22 April 1999)

The transport properties of the manganites $La_{1-x}Sn_xMnO_{3+\delta}$ with $x=0.1$–0.5 and of Fe-doped samples have been comprehensively studied using magnetoresistance measurements, ^{57}Fe and ^{119}Sn Mössbauer spectroscopy, and x-ray diffraction. At the Sn concentration $x=0.5$, $La_{0.5}Sn_{0.5}MnO_{3+\delta}$, is a single phase. The manganites $La_{1-x}Sn_xMnO_{3+\delta}$ with $x<0.5$ consist of two phases, ABO_3 and $A_2B_2O_7$; the chemical formulas are $LaMnO_{3+\delta}$ and $(La_{0.5}Sn_{0.5})_2Mn_2O_7$, respectively. The colossal magnetoresistance (CMR) in $La_{1-x}Sn_xMnO_{3+\delta}$ appears to have its origin in deficient La and/or Mn ions in the ABO_3 phase. Mössbauer spectra show that a superparamagnetic doublet exists from $T=250$–77 K for the ABO_3 phase in the Fe-doped sample and may have superparamagneticlike spin clusters that lead to a low saturation field. Consequently, the CMR reaches 75% at an applied field of only 20 kOe for the Fe-doped sample; however, the same CMR requires fields as high as 70 kOe in the undoped $La_{0.7}Sn_{0.3}MnO_{3+\delta}$ sample. [S0163-1829(99)02437-6]

I. INTRODUCTION

Generally, manganites with colossal magnetoresistance (CMR) can be classified into two categories. One is the perovskite-type compound (ABO_3) with a chemical formula $(R^{3+}_{1-x}D^{2+}_x)(Mn^{3+}_{1-x}Mn^{4+}_x)O_3$ (R=rare-earth and D=Ca, Sr, Ba, Pb, and Cd, all divalent).[1] The other is the pyrochlore-type compound ($A_2B_2O_7$) with the formula $Tl^{3+}_2Mn^{4+}_2O_7$.[2,3]

Recently, it has been discovered that $La_{0.7}Sn_{0.3}MnO_{3+\delta}$ exhibits CMR near room temperature. Its magnetoresistivity coefficient (classical) is as high as 74% for $H=70$ kOe.[4] Further investigation showed that this manganite consists of two phases; one is the perovskite-type ABO_3 and the other is the pyrochlore-type $A_2B_2O_7$.[5] Krivoruchko *et al.*[6] reported compositions of the two phases, $La_{0.4}\square_{0.6}MnO_{3-\delta}$ for the ABO_3 phase and $La_2Sn_2O_7$ for the $A_2B_2O_7$ phase. However, it is hard to believe that the perovskite structure can be maintained for so large a deficiency of La ions.

Fe doping can significantly modify the magnetic and transport properties of manganites.[7–9] An increase in CMR for Fe-doped samples has been reported in La-Ca-Mn-O systems[8] and La-Sn-Mn-O systems.[7] A metalliclike conductivity and ferromagnetic ground state for the perovskite compound $La_{1-x}M^{2+}_xMnO_3$ are attributed to the double-exchange model which involves electron exchange between neighboring Mn^{3+} and Mn^{4+} sites. The correlations between transport behavior and magnetic properties have been studied.[10–12] Some models, such as the Kondo model and the polaron model have been proposed to describe the correlations for the La-Sr-Mn-O and La-Ca-Mn-O systems. However, the origin of the increase in CMR for Fe-doped samples, as far as we know, has not been proposed up to now. In this work, based on our Mössbauer spectra, a superparamagneticlike model is proposed to describe the properties for Fe-doped La-Sn-Mn-O systems. In addition, the compositions of the two phases in La-Sn-Mn-O were determined by x ray as well as ^{57}Fe and ^{119}Sn Mössbauer spectra.

II. EXPERIMENTAL

Samples of $La_{1-x}Sn_xMnO_{3+\delta}$ with $x=0.1$, 0.2, 0.3, and 0.5 as well as Fe-doped $La_{1-x}Sn_xMn_{0.985}Fe^{57}_{0.015}O_{3+\delta}$ with $x=0.3$ and 0.5 were synthesized using conventional ceramic techniques. A mixture of oxides La_2O_3, SnO_2, MnO_2, and $^{57}Fe_2O_3$ of stoichometric composition was presintered at 800 °C for 10 h and then crushed. The samples were shaped and sintered in O_2 at 1200 °C for 6 h and followed by annealing at 900 °C for 24 h.

X-ray diffraction (XRD) was performed with a Philips diffractometer using Cu $K\alpha$ radiation. The magnetoresistances were examined at 4.2–300 K with zero field and up to 70 kOe applied field using the standard four-probe method. ^{57}Fe Mössbauer spectra from 4.2 K to room temperature and ^{119}Sn Mössbauer spectra at room temperature were taken with a conventional constant acceleration spectrometer. The γ-ray sources were ^{57}Co in a Rh matrix and ^{119}Sn in $BaSnO_3$. All isomer shifts are given relative to that of α-Fe at room temperature.

III. RESULTS

A. Magnetoresistance

1. CMR for La-Sn-Mn-O

The transport properties of $La_{1-x}Sn_xMnO_{3+\delta}$ ($x=0.1$, 0.2, 0.3, and 0.5) are shown in Table I. $La_{0.5}Sn_{0.5}MnO_{3+\delta}$ is an insulator; the other samples are electrical conductors. The resistivities at room temperature increase with Sn substitutions; they are 0.036, 0.064, and 0.20 Ω cm for the samples with Sn concentrations $x=0.1$, 0.2, and 0.3, respectively. The manganites $La_{1-x}Sn_xMnO_{3+\delta}$ have a semiconductor-metal transition (S-M transition) at 235–245 K. The maxi-

TABLE I. Transport properties of $La_{1-x}Sn_xMnO_{3+\delta}$.

x	$\rho(0)$ (Ω cm)	$\rho(H=0)$ (Ω cm)	$\rho(H=15$ kOe) (Ω cm)	MR (%) %	$T_{S\text{-}M}$ (K)
0.1	0.036	0.080	0.057	−29	245
0.2	0.064	0.150	0.115	−23	240
0.3	0.20	0.61	0.46	−25	235
0.3[a]	0.73	7.45	2.38	−74	195
0.5	Insulator				

[a]The Fe-doped sample.

mum magnetoresistance (MR) effect occurs at the transition temperatures, as shown in Fig. 1. The magnetoresistance coefficient, defined as

$$\mathrm{MR} = -\Delta\rho/\rho \times 100\% = [\rho(\mathrm{H,T}) - \rho(0,T)]/\rho(0,T) \times 100\%$$

in H = 15 kOe are 29, 23, and 25 % for the samples with $x = 0.1$, 0.2, and 0.3, respectively.

2. The effect of Fe doping on CMR

A small amount of Fe doping modifies the magnetoresistance of the La-Sn-Mn-O systems. First, the resistivity at room temperature is about triple and the maximum resistivity at the S-M transition temperature is over 10 times greater for the Fe-doped sample, $La_{0.7}Sn_{0.3}Mn_{0.985}Fe^{57}_{0.015}O_{3+\delta}$, than its parent. Second, the S-M transition temperature is reduced by 40 K, viz. from 235 K for $La_{0.7}Sn_{0.3}MnO_{3+\delta}$ to 195 K for the Fe-doped sample. Mössbauer spectra show that Fe moments are antiparallel to the Mn moments, as described in Sec. III C 2. The antiferromagnetic Fe-O-Mn superexchange interaction can weaken the double-exchange interaction between Mn^{3+} and Mn^{4+} ions, which leads to an increase in the resistivity and a decrease in the S-M transition temperature.

More importantly, Fe doping can reduce the saturation field of the magnetoresistance effect. Figure 2 shows the dependence of MR on the applied fields H for

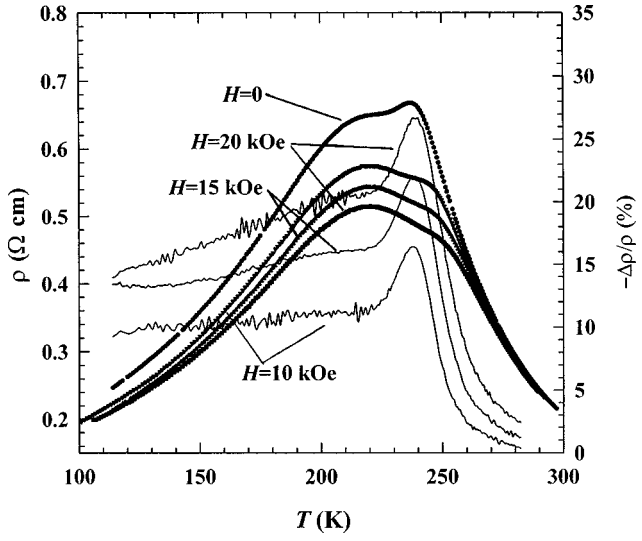

FIG. 1. Resistivity-temperature curves (solid points) in zero as well as 10, 15, and 20 kOe applied field and the corresponding magnetoresistance coefficient-temperature curves (solid line) for $La_{0.7}Sn_{0.3}MnO_{3+\delta}$.

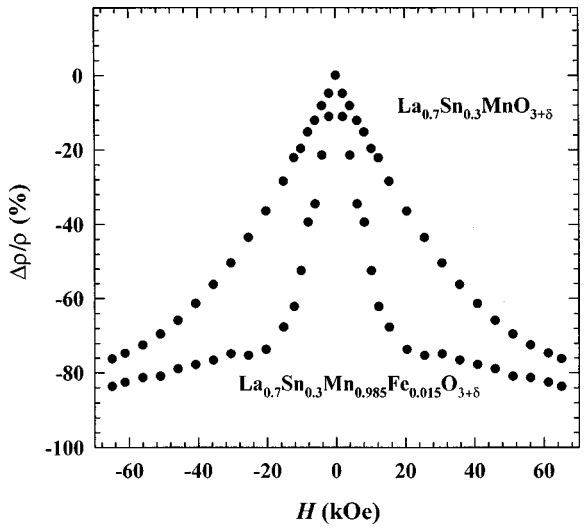

FIG. 2. The magnetoresistance coefficient-applied field curves at S-M transition temperature, $T_{S\text{-}M} = 235$ K and 195 K for $La_{0.7}Sn_{0.3}MnO_{3+\delta}$ and $La_{0.7}Sn_{0.3}Mn_{0.985}Fe_{0.015}O_{3+\delta}$, respectively.

$La_{0.7}Sn_{0.3}MnO_{3+\delta}$ and $La_{0.7}Sn_{0.3}Mn_{0.985}Fe^{57}_{0.015}O_{3+\delta}$. For $La_{0.7}Sn_{0.3}MnO_{3+\delta}$, the MR does not reach saturation even if the field is as high as 70 kOe. However, for the Fe-doped sample, at $H = 20$ kOe, the MR is close to saturation. Consequently, although in a high field the MR is almost the same for both, in a low field such as $H = 20$ kOe, the MR is much superior for the Fe-doped sample than for its parent $La_{1-x}Sn_xMnO_{3+\delta}$. The MR is as large as 75% at the applied field of 20 kOe for the Fe-doped sample; however, to obtain the same MR, a field at as high as 70 kOe is required for $La_{0.7}Sn_{0.3}MnO_{3+\delta}$.

B. X-ray diffraction

The x-ray diffraction (XRD) patterns for $La_{1-x}Sn_xMnO_{3+\delta}$ with $x = 0.1$, 0.2, 0.3, and 0.5 are shown in Fig. 3. The lattice parameters are listed in Table II. Only the sample with $x = 0.5$ is a single phase that has the cubic structure. The positions and intensities of the XRD are similar to those for $La_2Sn_2O_7$ (Ref. 13) and $Tl_2Mn_2O_7$.[3] The other samples ($x = 0.1$, 0.2, and 0.3) are mixtures of the two phases. One is $A_2B_2O_7$; the other is ABO_3 with the monoclinic or rhombohedral structure, respectively, similar to $La_{0.8}Sr_{0.2}MnO_3$ (Ref. 14) or $La_{2/3}Pb_{1/3}MnO_3$. However, the double rhombohedral structure[15] is excluded because the (113) XRD line is not observed. In Fig. 3, the indexing is based on the monoclinic structure. With increasing Sn concentration, the intensities of the XRD decrease for ABO_3 and increase for $A_2B_2O_7$.

In order to obtain the volume fraction for the two phases, a series of mixtures of $(La_{0.5}Sn_{0.5})_2Mn_2O_7$ and $LaMnO_3$ with known weight fractions were made. The intensities of (440) XRD lines in $A_2B_2O_7$ and of (220) lines in ABO_3 were measured. The intensity ratios as a function of the volume fractions or weight fractions, were plotted. Based on the standard curve, the volume fractions of ABO_3 and $A_2B_2O_7$ are obtained for $La_{1-x}Sn_xMnO_{3+\delta}$ and the results are also listed in Table II.

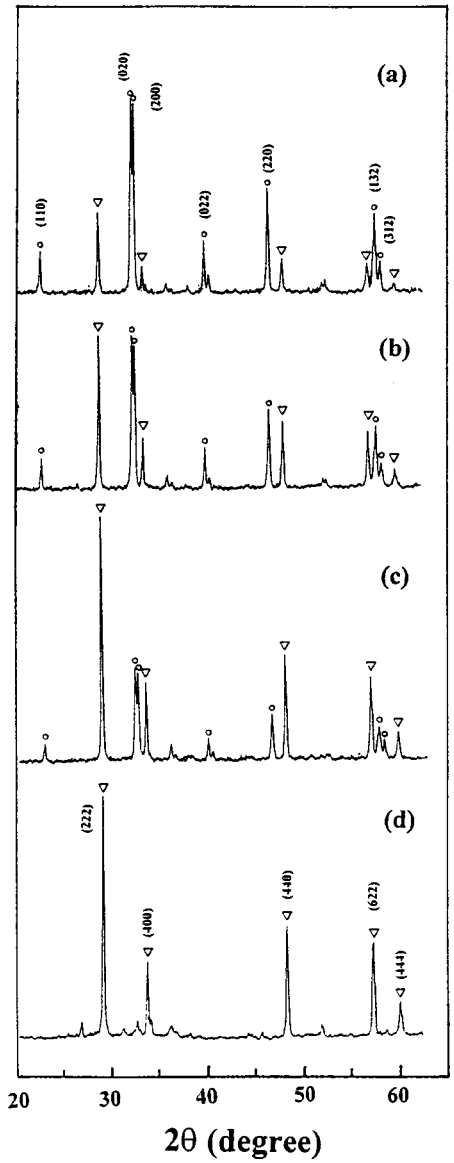

FIG. 3. X-ray-diffraction patterns for $La_{1-x}Sn_xMnO_{3+\delta}$ with (a) $x=0.1$, (b) $x=0.2$, (c) $x=0.3$, and (d) $x=0.4$. The circles and triangles represent the ABO_3 and $A_2B_2O_7$ phases, respectively.

C. Mössbauer spectra

1. ^{57}Fe and ^{119}Sn Mössbauer spectra at room temperature

^{57}Fe Mössbauer spectra of $La_{1-x}Sn_xMn_{0.985}Fe_{0.015}O_{3+\delta}$ with $x=0.3$ and 0.5 at room temperature are shown in Fig. 4. Fitted hyperfine parameters are listed in Table III. The spectrum of sample with $x=0.5$ is a doublet; the isomer shift and quadrupole splitting are 0.35 and 1.47 mm/s, respectively. The spectrum of sample with $x=0.3$ consists of two doublets.

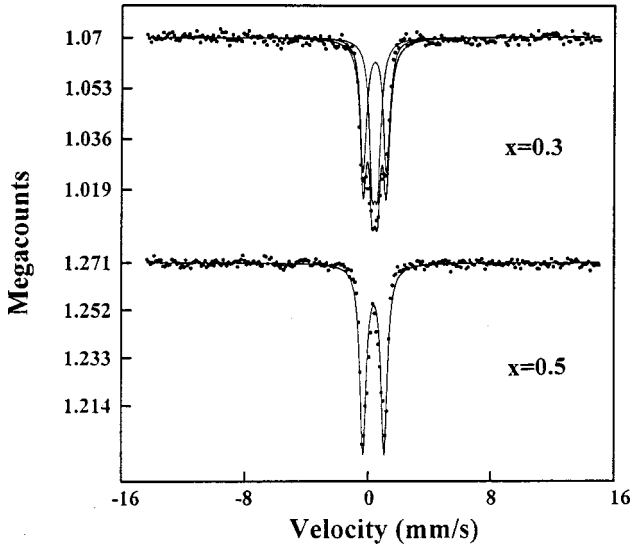

FIG. 4. ^{57}Fe Mössbauer spectra at room temperature for $La_{1-x}Sn_xMn_{0.985}Fe_{0.015}O_{3+\delta}$ with $x=0.3$ and 0.5.

For the outer one, the isomer shift and quadrupole splitting are 0.36 and 1.51 mm/s, respectively, almost the same as the sample with $x=0.5$. This doublet is assigned to the $A_2B_2O_7$ phase. For the inner one, the isomer shift and quadrupole splitting are 0.37 and 0.38 mm/s; this doublet is assigned to the ABO_3 phase. The values of isomer shifts (0.35–0.38 mm/s) indicate that all Fe ions are in the ferric (Fe^{3+}) state for the two phases.

^{119}Sn Mössbauer spectra of $La_{1-x}Sn_xMnO_{3+\delta}$ with $x=0.3$ and 0.5 at room temperature consist of one doublet, as shown in Fig. 5. Both have almost the same isomer shift and quadrupole splitting. The isomer shifts are 0.15(2) and 0.16(2) mm/s and the quadrupole splittings are 0.52(2) and 0.65(2) mm/s, respectively, for the samples with $x=0.3$ and 0.5. It is known that the range of isomer shifts are 0.00–1.30 for Sn^{4+} and 2.30–4.44 mm/s for Sn^{2+}. Hence, the isomer shift of 0.15 mm/s implies that all Sn ions are in the 4+ valence state for the samples with $x=0.3$ and 0.5.

2. ^{57}Fe Mössbauer spectra at 4.2 K

Mössbauer spectra of $La_{1-x}Sn_xMn_{0.985}Fe_{0.015}O_{3+\delta}$ ($x=0.3$ and 0.5) at $T=4.2$ K are shown in Fig. 6 and the fitted

TABLE II. Structure parameters of $La_{1-x}Sn_xMnO_{3+\delta}$.

x	Phase	a (Å)	b (Å)	c (Å)	Angle (°)	V_{exp} (%)	V_{cal} (%)
0.1	ABO_3	5.504(4)	5.538(3)	7.838(8)	91.1(1)	22	24
	$A_2B_2O_7$	10.724(9)				78	76
0.2	ABO_3	5.500(2)	5.541(1)	7.839(13)	91.0(1)	45	46
	$A_2B_2O_7$	10.722(9)				55	54
0.3	ABO_3	5.491(3)	5.538(2)	7.822(9)	90.8(1)	63	66
	$A_2B_2O_7$	10.716(7)				37	34
0.5	$A_2B_2O_7$	10.728(10)					

TABLE III. ^{57}Fe and ^{119}Sn Mössbauer parameters of $La_{1-x}Sn_xMn_{0.985}Fe_{0.015}O_{3+\delta}$ ($x=0.3$ and 0.5) at $T=300$ K. Here, δ is the isomer shift with respect to α-Fe, ϵ is the quadrupole splitting, Γ is the linewidth, and S is the relative area.

Sample	Phase	δ (mm/s)	ϵ (mm/s)	Γ (mm/s)	S (%)
			^{57}Fe		
$x=0.5$	$A_2B_2O_7$	0.35(3)	1.47(3)	0.49	100
$x=0.3$	$A_2B_2O_7$	0.36	1.51	0.42	48.3
	ABO_3	0.38	0.36	0.42	51.7
			^{119}Sn		
$x=0.5$	$A_2B_2O_7$	0.15(3)	0.52(3)	1.27	100
$x=0.3$	$A_2B_2O_7$	0.16(3)	0.65	1.42	100

hyperfine parameters are listed in Table IV. The Mössbauer spectrum of $La_{0.5}Sn_{0.5}Mn_{0.985}Fe_{0.015}O_{3+\delta}$ is a sextet. The hyperfine field is 474 kOe. The Mössbauer spectrum of $La_{0.7}Sn_{0.3}Mn_{0.985}Fe_{0.015}O_{3+\delta}$ consists of two sextets. The hyperfine fields are 474 and 525 kOe, corresponding to the phases $A_2B_2O_7$ and ABO_3, respectively.

After a longitudinal magnetic field of 50 kOe was applied, for ABO_3, the second and fifth lines disappear and, as compared to 525 kOe in zero applied field, the hyperfine field (576 kOe) increases by 51 kOe, which is almost the same as the value of the applied field. This means that the Fe moments are collinear but antiparallel with the Mn moments.

However, for $A_2B_2O_7$, the Mössbauer spectrum is still a sextet without line broadening; therefore antiferromagnetic coupling between the Fe moments is excluded. The nonzero second and fifth lines imply that Fe moments are canted with ferromagnetic coupling or are in a spin-glass state, although ac susceptibility has shown that Mn ions have antiferromagnetic arrangements.[7] The hyperfine field is 514 kOe, larger by 40 kOe as compared to the hyperfine field with zero applied field.

3. ^{57}Fe Mössbauer spectra between $T=300$ and 4.2 K

Mössbauer spectra of $La_{1-x}Sn_xMn_{0.985}Fe_{0.015}O_{3+\delta}$ with $x=0.3$ and 0.5 between $T=300$ and 4.2 K have been collected. The Mössbauer spectra of the sample with $x=0.5$ are a paramagnetic doublet from room temperature to 65 K. The doublet starts to disappear and becomes a sextet between 65 and 50 K. Therefore, the magnetic ordering temperature is between 65 and 50 K.

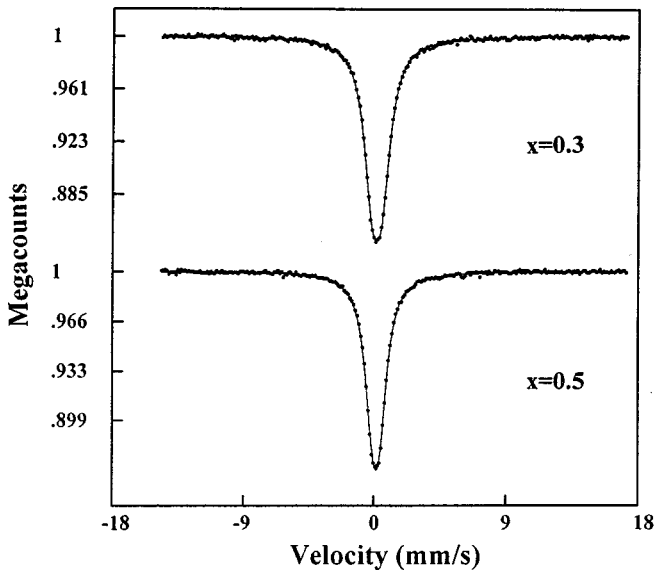

FIG. 5. ^{119}Sn Mössbauer spectra at room temperature for $La_{1-x}Sn_xMn_{0.985}Fe_{0.015}O_{3+\delta}$ with $x=0.3$ and 0.5.

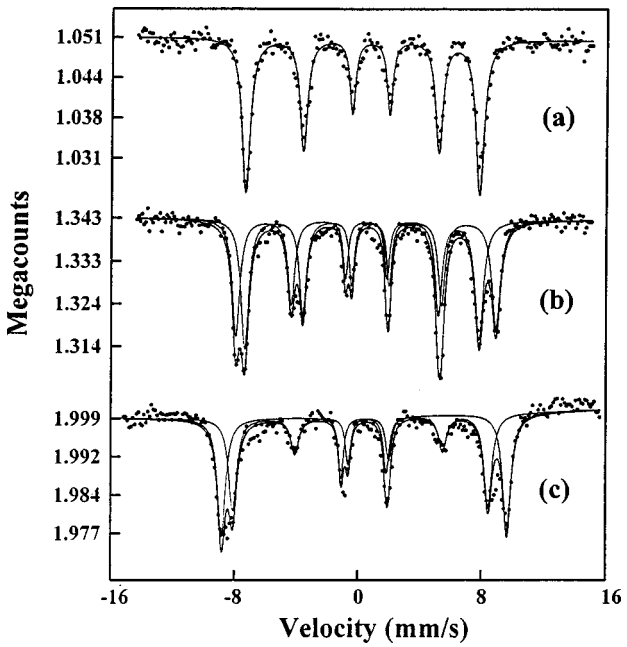

FIG. 6. At $T=4.2$ K ^{57}Fe Mössbauer spectra of (a) $La_{0.5}Sn_{0.5}Mn_{0.985}Fe_{0.015}O_{3+\delta}$ and of $La_{0.7}Sn_{0.3}Mn_{0.985}Fe_{0.015}O_{3+\delta}$ (b) in zero field and (c) in a longitudinal applied field of 50 kOe.

The Mössbauer spectra of the sample with $x=0.3$ between 300 and 4.2 K are shown in Fig. 7. At room temperature two paramagnetic doublets are observed. The inner doublet (ABO_3) starts to become a mixture of a doublet and a sextet below 250 K. However, the outer doublet ($A_2B_2O_7$) remains until $T=65$ K. Only below 65 K does the outer doublet disappear and spectra consist of two sextets. Therefore, $La_{0.7}Sn_{0.3}Mn_{0.985}Fe_{0.015}O_{3+\delta}$ has two transitions which occur at $T=250$ and 65 K, respectively; the result is supported by ac susceptibility data.[7] In addition, the spectra of ABO_3 exhibit a superparamagneticlike character, described in detail by Sec. IV.

TABLE IV. ^{57}Fe Mössbauer parameters of $La_{1-x}Sn_xMn_{0.985}Fe_{0.015}O_{3+\delta}$ ($x=0.3$ and 0.5) in zero and a 50 kOe applied field at $T=4.2$ K. Here, δ is the isomer shift with respect to α-Fe, ϵ is the quadrupole splitting, H_{hf} is the hyperfine field, b is the area ratio of the second plus fifth to the third plus fourth and S is the relative area.

Sample	Phase	δ (mm/s)	ϵ (mm/s)	H_{hf} (kOe)	b	S (%)
			$H_a=0$ kOe			
$x=0.5$	$A_2B_2O_7$	0.50(3)	$-0.46(3)$	474(3)	2.0	100
$x=0.3$	$A_2B_2O_7$	0.51	-0.64	474	2.0	47.4
	ABO_3	0.50	0.03	525	2.0	
			$H_a=50$ kOe			
$x=0.3$	$A_2B_2O_7$	0.47(3)	$-0.41(3)$	514(3)	1.30	50.1
	ABO_3	0.56	0.04	576	0.0	49.9

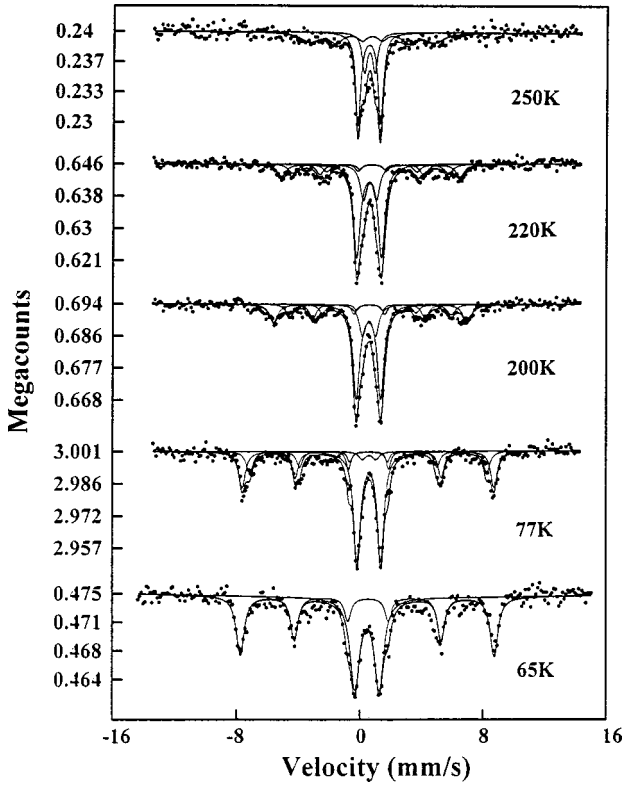

FIG. 7. ^{57}Fe Mössbauer spectra from 250 to 65 K for $La_{0.7}Sn_{0.3}Mn_{0.985}Fe_{0.015}O_{3+\delta}$.

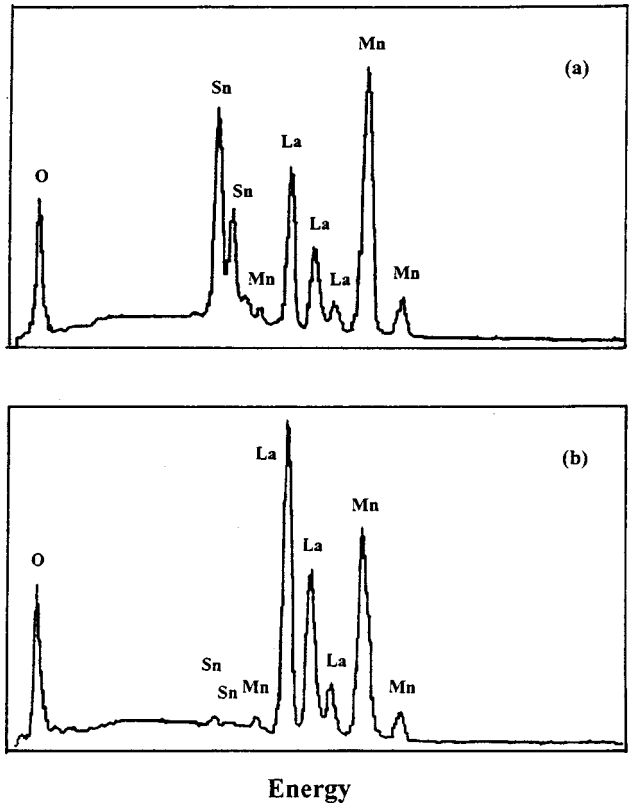

FIG. 8. Energy-dispersive spectra (0–10.24 keV) for $La_{0.9}Sn_{0.1}MnO_{3+\delta}$; the percentage of La, Sn, and Mn atoms is (a) 21.9:24.9:53.2 and (b) 48.6:1.6:49.8 corrected for atomic number effect, absorption of x rays within the specimen, and fluoresence effects (the ZAF technique).

IV. DISCUSSION

A. Phase compositions

The ^{57}Fe Mössbauer spectrum at room temperature has two subspectra for $La_{0.7}Sn_{0.3}Mn_{0.985}Fe_{0.015}O_{3+\delta}$ and only one for $La_{0.5}Sn_{0.5}Mn_{0.985}Fe_{0.015}O_{3+\delta}$. This shows that Mn(Fe) ions are located in two phases for the sample with $x=0.3$ and only one in the $A_2B_2O_7$ phase for the sample with $x=0.5$ (Fig. 4). However, ^{119}Sn Mössbauer spectra at room temperature have only one component for both samples. Further, isomer shifts and quadrupole splittings are almost the same, as shown in Sec. III B 1. This shows that the Sn ions are only in the $A_2B_2O_7$ phase.

It is known that the ion radii are much larger for La^{3+} (1.032 Å) than for Sn^{4+} (0.69 Å). Consequently, with Sn substitution for La the lattice parameters should have been significantly reduced. However, XRD results show that when the Sn concentrations change from 0.1 to 0.5 the lattice parameters are almost constant within the experimental errors for $A_2B_2O_7$ and ABO_3. This implies that the phase compositions are the same in each phase for all samples.

Quantitative analysis of XRD is also able to confirm that the Sn ions are located in $A_2B_2O_7$. It is supposed that all Sn ions are in $A_2B_2O_7$ and none are in ABO_3; in other words, the chemical formulas are $LaMnO_{3+\delta}$ and $(La_{0.5}Sn_{0.5})_2Mn_2O_7$ for the ABO_3 and $A_2B_2O_7$ phases, respectively. The relative amounts, C_{227} and C_{113}, of the two phases can be obtained from the Sn concentration x, the cell volumes V_{227} and V_{113}, and the cell number per chemical formula N_{227} and N_{113},

$$\frac{C_{227}}{C_{113}}=\frac{x}{1-2x}\frac{V_{227}/N_{227}}{V_{113}/N_{113}}, \tag{1}$$

where the volumes are $V_{227}=1232$ Å and $V_{113}=239$ Å, determined by the lattice parameters, and $N_{227}=8$ and $N_{113}=4$ based on the crystal structures. The calculated results are C_{227}: $C_{113}=24{:}76$, $46{:}54$, and $66{:}34$ for the samples with $x=0.1$, 0.2, and 0.3, respectively. These ratios are very consistent with the values obtained from quantitative analysis of XRD, as shown in Table II.

Energy dispersive spectroscopy (EDS) quantitative analysis also indicated the concentrations of La, Sn, and Mn averaged over many grains are very close to the formula $La_{1-x}Sn_xMnO_{3+\delta}$ for all samples. A homogeneous composition distribution of La, Sn, and Mn is observed everywhere for $La_{0.5}Sn_{0.5}MnO_{3+\delta}$. However, it was found that for the other samples with $x=0.1$, 0.2, and 0.3 there exist two kinds of grains in which the compositions are significantly different. For one, the quantity of La plus Sn ions is close to that of Mn ions; for the other grain, there is an equal number of La and Mn ions but almost no Sn ion as shown in Fig. 8.

Based on the XRD, EDS, and Mössbauer spectra, the manganites $La_{1-x}Sn_xMnO_{3+\delta}$ with $x=0.1$, 0.2, and 0.3 are a mixture of two phases, ABO_3 and $A_2B_2O_7$; the formulas are $LaMnO_{3+\delta}$ and $(La_{0.5}Sn_{0.5})_2Mn_2O_7$, respectively. The amount of the two phases is dependant on the Sn concentrations. With increasing Sn substitution, the amount of ABO_3 decreases and that of $A_2B_2O_7$ increases. Therefore, the maximum magnetoresistance coefficient and the S-M transition temperature are roughly the same for all the samples with Sn concentration $x=0.1$, 0.2, and 0.3; but the resistivities become large with increasing Sn substitution. In addition, at the

Sn concentration $x=0.5$, $(La_{0.5}Sn_{0.5})_2Mn_2O_7$ is a single phase.

The CMR and S-M transition in $La_{1-x}Sn_xMnO_{3+\delta}$ occurs at $T=235$–245 K. The ABO_3 phase has a magnetic transition at about 240 K. Consequently, the CMR in $La_{1-x}Sn_xMnO_{3+\delta}$ with $x=0.1$, 0.2, and 0.3 is associated with the ABO_3 phase. It is known that $LaMnO_3$ is an antiferromagnetic insulator. However, a deficiency of La and/or Mn ions can lead to a CRM. Results of the CMR in $La_{1-x}MnO_3$ and $LaMnO_{3+\delta}$ have been reported recently.[16–18] Our work also indicates that $La_{0.9}MnO_{3+\delta}$ has a S-M transition at $T=240$ K, a paramagnetic-ferromagnetic transition at $T=250$ K, and the CMR is about 26% in $H=15$ kOe at $T=240$ K.[19] Hence, the CMR in $La_{1-x}Sn_xMnO_{3+\delta}$ may have its origin in a deficiency of La and/or Mn ions for the ABO_3 phase.

B. Superparamagneticlike behavior and CMR

Between the temperature range of 250 and 65 K, the Mössbauer spectra of the ABO_3 phase ($LaMnO_{3+\delta}$) in $La_{0.7}Sn_{0.3}Mn_{0.985}Fe_{0.015}O_{3+\delta}$ can be fitted with three subspectra, as shown in Fig. 7. One is a doublet; the others are sextets. One sextet is expected when Fe ions substitute for the Mn ions which occupy only one site in the perovskite structure; the other may have one or more sources, viz (a) Fe ions in a defect structure produced by the deficiency of La-Mn ions, (b) near the surface[15] and (3) perhaps with different numbers of Fe-Mn neighbors. In addition, the Curie temperature is 235 K for $La_{0.7}Sn_{0.3}Mn_{0.985}Fe_{0.015}O_{3+\delta}$.[4] However, a hyperfine field at $T=250$ K was observed above the Curie temperature, as shown in Figs. 7 and 9(d). A similar observation in the La-Sr-Mn(Fe)-O system was also reported by Tkachuk *et al.*[20] The hyperfine fields above the Curie temperature may be attributed to sample inhomogeneity or to a formation of local ferromagnetic clusters at Fe sites.[20]

The spectra of $LaMn(Fe)O_{3+\delta}(ABO_3)$ exhibit the following superparamagnetic characteristics. (1) The spectra consist of a doublet and two sextets. With decreasing temperatures, the relative areas of the sextets gradually increase whereas that of the doublet gradually decreases to zero below $T=65$ K, as shown in Fig. 9(a). (2) The quadrupole splittings of the doublet between 220 and 65 K are approximately constant and significantly different from that at room temperature (in the paramagnetic state), as shown in Fig. 9(b). (3) The fitted linewidth is approximately the same for either the sextets or the doublet, except for the linewidth at $T=250$ K, as shown in Fig. 9(c). The linewidths of $LaMn(Fe)O_{3+\delta}$ are significantly different from those of La-Ca-Mn(Fe)-O and La-Sr-Mn(Fe)-O in which line broadening of the sextets has been observed with increasing temperatures.[20,21] The broadening was interpreted using a model based either on an antiferromagnetic impurity in a ferromagnetic host[21] or on spin fluctuations.[20]

However, the particle sizes of the sample are of the order of micrometers based on observations with optical microscopy. Further, line broadening is not observed in x-ray-diffraction patterns. These results exclude the possibility of superparamagnetism produced by ultrafine particles. Perhaps, the superparamagnetism has its origin in superparamagneticlike spin clusters at Fe sites.[22]

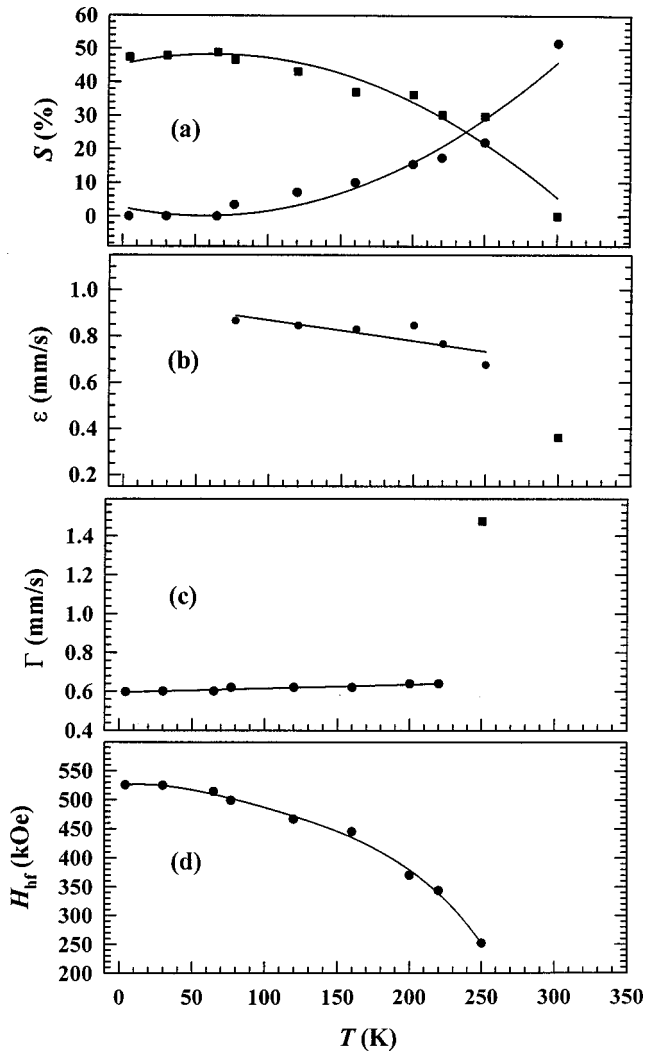

FIG. 9. Some Mössbauer parameters of the ABO_3 phase for sample $La_{0.7}Sn_{0.3}Mn_{0.985}Fe_{0.015}O_{3+\delta}$, (a) the relative areas for the doublet (circles) and the sextet (squares), (b) the quadrupole splittings for the doublet, (c) linewidth for the sextet, and (d) hyperfine field for the sextet.

The dependence of $\Delta\rho/\rho(0)$ on the applied field H can be fitted using a Langevin function

$$\Delta\rho(H)/\rho(0) = -\beta[\coth(\alpha) - 1/\alpha], \tag{2}$$

where $\alpha = N\mu_B H/kT$, μ_B is the Bohr magneton, and k is Boltzmann's constant. N and β are fitted parameters. N is the average number of spin in a superparamagneticlike cluster, namely, the average size of the clusters. β is the maximum MR as $H\rightarrow\infty$ at a certain temperature. The fitted curves are shown in Fig. 10. Obviously, the experimental $\Delta\rho/\rho(0)$ is very consistent with the Langevin curves. The behavior of the magnetoresistance in applied fields is related to the average spin numbers in a cluster, namely the average size of a cluster. When the temperature drops, the size of a cluster decreases and the CMR also decreases.

In this work, no evidence was found as to whether the sample without Fe doping, $La_{0.7}Sn_{0.3}MnO_{3+\delta}$, has a superparamagneticlike spin clusters. This is an interesting problem that will be further studied.

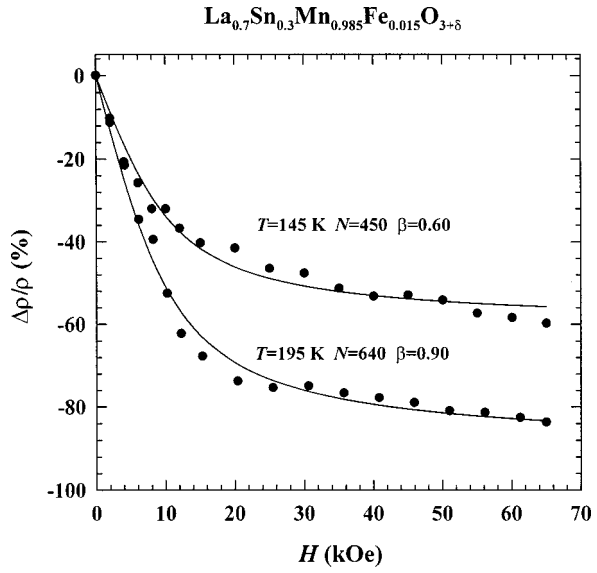

FIG. 10. The magnetoresistance coefficient-applied field curves for $La_{0.7}Sn_{0.3}Mn_{0.985}Fe_{0.015}O_{3+\delta}$ and the fitting curves based on a Langevin function.

According to the double-exchange model, the resistivity depends on electron-spin alignment of the hopping electron and is decreased by applying a magnetic field or by reducing the temperatures that reduce the spin disorder. As compared to $LaMnO_{3+\delta}$, doping with Fe has two additional effects. Mössbauer spectrum with an applied field of 50 kOe has shown that all Fe moments are collinear but antiparallel with the Mn moments. Antiferromagnetic Fe-O-Mn superexchange interactions would weaken the double-exchange interaction between Mn^{3+} and Mn^{4+} ions, as described by Leung *et al.*[15] On the other hand, the superparamagneticlike clusters also lead to an increase in electronic scattering below T_C. Consequently, the resistivity is ten times higher for the Fe-doped sample than for $La_{0.7}Sn_{0.3}MnO_{3+\delta}$ (see Table I). When the magnetic field is applied, the superparamagneticlike clusters are destroyed and the spins tend to alignment along the field. As a result, the resistivity decreases rapidly.

V. CONCLUSIONS

Based on the XRD, EDS, and ^{57}Fe and ^{119}Sn Mössbauer spectra, at the Sn concentration $x=0.5$, $La_{1-x}Sn_xMnO_{3+\delta}$ is a single phase $(La_{0.5}Sn_{0.5})_2Mn_2O_7$. At Sn concentrations $x<5$, the manganites $La_{1-x}Sn_xMnO_{3+\delta}$ have two phases. One is ABO_3 with the chemical formula $LaMnO_{3+\delta}$ and the other is $A_2B_2O_7$ with the formula $(La_{0.5}Sn_{0.5})_2Mn_2O_7$. The CMR in $La_{1-x}Sn_xMnO_{3+\delta}$ seems to have its origin in the deficient La and/or Mn ions in the ABO_3 phase.

The transport properties of $La_{1-x}Sn_xMnO_{3+\delta}$ are modified by Fe doping, which leads to a low saturation field for magnetoresistance, a decrease in the S-M transition temperature and an increase in the resistivity. Mössbauer spectra also indicated that the superparamagnetic doublet persists from $T=250$ K to 77 K for the ABO_3 phase in the Fe-doped sample. The low saturation field may be related to superparamagneticlike spin clusters. Consequently, the CMR reaches 75% at an applied field of only 20 kOe for the Fe-doped sample; however, the same CMR requires field as high as 70 kOe for $La_{0.7}Sn_{0.3}MnO_{3+\delta}$.

ACKNOWLEDGMENTS

The financial support of the Natural Sciences and Engineering Research Council of Canada is acknowledged. The authors thank J.H. Zhao and X. Z. Zhou for assistance with the CMR measurements.

[1] S. Jin, H.M. O'Bryan, T.H. Tiefel, M. McCormack, and W.W. Rhodes, Appl. Phys. Lett. **66**, 382 (1990).
[2] Y. Shimakawa, Y. Kubo, and T. Manako, Nature (London) **379**, 53 (1996).
[3] M.A. Subramanian, B.H. Toby, A.P. Ramirez, W.J. Marshall, A.W. Sleight, and G.H. Kwei, Science **273**, 81 (1996).
[4] S. Dai, Z.W. Li, A.H. Morrish, X.Z. Zhou, J.G. Zhao, and X.M. Xiong, Phys. Rev. B **55**, 14 125 (1997).
[5] A.H. Morrish, Z.W. Li, S. Dai, X.Z. Zhou, J.G. Zhao, and X.M. Xiong, Hyperfine Interact. **113**, 485 (1998).
[6] V.N. Krivoruchko, V.P. Pashchenko, Yu V. Medverdev, S.L. Khartsev, A.A. Shemyakov, M.M. Savosta, V.I. Kamenev, A.D. Loyko, G.K. Volkova, and V.I. Volkov, Phys. Lett. A **245**, 163 (1998).
[7] Z.W. Li, A.H. Morrish, and X.Z. Zhou, J. Appl. Phys. **83**, 7198 (1998).
[8] L. Righi, P. Gorria, M. Insausti, J. Guitierrez, and J.M. Barandiaran, J. Appl. Phys. **81**, 5767 (1997).
[9] K.H. Ahn, X.W. Wu, K. Liu, and C.L. Chien, Phys. Rev. B **54**, 15 299 (1996).
[10] Y. Tokura, A. Urushibara, Y. Moritomo, T. Arima, A. Asamitsu, G. Kido, and N. Furukawa, J. Phys. Soc. Jpn. **63**, 3931 (1994).
[11] D. Emin and N.L.H. Liu, Phys. Rev. B **27**, 4788 (1983).
[12] M.H. Hundley, M. Hawley, R.H. Heffiner, Q.X. Jia, J.J. Neumeier, J. Tesmer, J.D. Thompson, and X.D. Wu, Appl. Phys. Lett. **67**, 860 (1995).
[13] C.G. Whinfrey, D.W. Eckart, and A. Tauber, J. Am. Chem. Soc. **82**, 2695 (1960).
[14] T. Hashimoto, J. Cryst. Growth **84**, 207 (1987).
[15] L.K. Leung, A.H. Morrish, and B.J. Evans, Phys. Rev. B **13**, 4069 (1976).
[16] M. Verels, N. Rangavittal, C.N.R. Rao, and A. Rousset, J. Solid State Chem. **104**, 74 (1993).
[17] T.R. McGuire, A. Gupta, P.R. Duncombe, M. Rupp, J.Z. Sun, R.B. Laibowitz, and W.J. Gallagher, J. Appl. Phys. **79**, 4549 (1996).
[18] A. Maignan, C. Michel, M. Hervieu, and B. Raveau, Solid State Commun. **101**, 277 (1996).
[19] Z. W. Li and A. H. Morrish (unpublished).
[20] A. Tkachuk, K. Rogacki, D.E. Brown, B. Dabrowski, A.J. Fedro, C.W. Kimball, B. Pyles, X. Xiong, D. Rosenmann, and B.D. Dunlap, Phys. Rev. B **57**, 8509 (1998).
[21] A. Simopoulos, M. Pissas, G. Kallias, E. Devlin, N. Moutis, I. Panagiotopoulos, D. Niarchos, C. Christides, and R. Sonntag, Phys. Rev. B **59**, 1263 (1999).
[22] D. Barlett, F. Tsui, D. Glick, L. Lauhon, T. Mandrekar, C. Uher, and R. Clarke, Phys. Rev. B **49**, 1521 (1994).